Supporting information for

Machine learning accelerated nitrogen electrofixation on dual-atom catalysts

Changfa Li,[a] Minmin Yan,[a] Pengchen Bao, [a] Jongkook Hwang,[b,c] Jingjing Duan,[a] Sheng Chen[a]**

[a]Key Laboratory for Soft Chemistry and Functional Materials, School of Chemistry and Chemical Engineering, School of Energy and Power Engineering, Nanjing University of Science and Technology, Ministry of Education, Nanjing, 210094, China

[b]Department of Chemical Engineering, Ajou University, Worldcupro 206, Suwon 16499, Republic of Korea

[c]Department of Energy Systems Research, Ajou University, Worldcupro 206, Suwon 16499, Republic of Korea

Email: jongkook@ajou.ac.kr (J.H.); sheng.chen@njust.edu.cn (S.C.)

Computational details

Electrochemical nitrogen reduction reaction (eNRR) catalyzed by transition metal atoms deposited on $MoSe_2$ sheets has been examined by density functional theory (DFT) through Perdew-Burke-Ernzerh of (PBE)[1] functional within the generalized gradient approximation (GGA) implemented in *MedeA* VASP.[2, 3] The projector-augmented-wave (PAW) pseudopotential was performed to treat the core-electron interactions.[4] A Gaussian smearing method was employed with 0.50 eV width. The K-points for structural optimization in all models were set to 2×2×1. The $MoSe_2$ (002) surface was cleaved across a direction to form a slab based on P63/mmc space group. Two-layer slab of $MoSe_2$ was used which was periodic on both the x and y directions consisting of 5×5 unit cells. The associated structural configurations are formed by $MoSe_2$ connected to two transition metal atoms though optimization with minimum energy. In preliminary works of pursuing efficiency, the cut-off energy for plane wave expansion was fixed at 400 eV, optimized from a range of cut-off energy; the electronic self-consistent-loop criterion was set to 10^{-2} eV and the structures were relaxed to forces on all atoms smaller than 0.02 eV/Å. In later verification of pursuing accuracy, the cut-off energy for plane wave expansion was fixed at 500 eV, optimized from a range of cut-off energy; the electronic self-consistent-loop criterion was set to 10^{-5} eV and the structures were relaxed to forces on all atoms smaller than 0.01 eV/Å; considering the DFT method has limitations in describing localized *d* electrons, we introduced the method of LSDA + U[5] and considered the effective U parameter (U_{eff}) of the Mo atom to be 1.0 eV [6, 7]for simplicity.

The detailed Gibbs free energy calculation without the extra potential was calculated has been carried out based on the computational hydrogen electrode (CHE) model proposed by Nørskov *et al.*[8] as follows:

$$G = E + \int C_P dT - TS + ZPE + D$$

where G, E and C_P refer to the chemical potential (partial molar Gibbs free energy), electronic energy and heat capacity, and T, S, ZPE and D refer to room temperature (298.15 K), the entropy, intrinsic zero-point energy and extrinsic dispersion, respectively. The entropy term can be expressed as the sum of the translational, rotational, vibrational and electronic contributions as to:

$$S = S_t + S_r + S_v + S_e$$

Since $S_e \approx 0$ at the fundamental electronic level. For the case of solids and adsorbates, some approximations can be assumed:

1. As for gases, at the fundamental electronic level $S_e \approx 0$.

2. Translational and rotational motions can be neglected, therefore, $S_t \approx 0$ and $S_r \approx 0$. In this sense, all entropy contributions come from vibrations: $S = S_v$. Similarly, translational and rotational contributions to the heat capacity are neglected.

Therefore, Gibbs free energy for the different states have been calculated as to:

$$G = E + \int C_P dT - TS_v + ZPE + D$$

The NRR is a six-electron reaction including six intermediate steps with electron transfer, N_2 adsorption and NH_3 desorption. For the instance of the distal mechanism, there are changes of intermediates in one nitrogen reduction reaction:

$$* + N_2 + 6H^+ \rightarrow *N_2 + 6H^+ \rightarrow *N_2H + 5H^+ \rightarrow *NNH_2 + 4H^+ \rightarrow *N + NH_3 + 3H^+ \rightarrow *NH + NH_3 + 2H^+ \rightarrow *NH_2 + NH_3 + H^+ \rightarrow *NH_3 + NH_3 \rightarrow 2NH_3$$

Where * and *X refer to the active site of catalysts and the intermediate with the adsorption of X. Therefore, the adsorption of NH_2, $E_{ads}(NH_2)$, have been calculated as to:

$$E_{ads}(NH_2) = G(*NH_2) + G(NH_3) + 1/2G(H_2) - [G(*) + G(N_2) + 3G(H_2)]$$

Where Gibbs free energy of micro molecules have been calculated as to:

$$G = E + H - TS + ZPE$$

Where the values of E is from www.atomly.net/, the values of H, enthalpy, is from https://janaf.nist.gov/, the values of TS and ZPE, have referred to the previous study[9]. Therefore, the energy change from NH_2 to NH_3 has been calculated as to:

$$\Delta G\,(NH_2\text{-}NH_3) = E_{ads}\,(NH_3) - E_{ads}\,(NH_2)$$

The free energy changes of other steps and adsorption energy of other intermediates follow the above-mentioned calculation method.

Machine-learning details

Machine learning (ML) is a critical branch of artificial intelligence (AI) that enables computers to learn from data automatically through computational methods, improving their decision-making or predictive accuracy over time without relying on pre-established equation models. ML algorithms consist of a series of statistical processing steps trained to identify natural patterns in the input data and make decisions and predictions based on these patterns.

Building a comprehensive ML process typically involves four key steps: first, selecting and preparing a training dataset; second, choosing an appropriate algorithm based on the nature of the problem; third, training the selected algorithm to create a model; and finally, testing and continuously refining the model. Common ML algorithms which were employed in the work mainly include:

1. Bagging regression[10] is a specific application of the bagging ensemble method tailored for regression tasks. It aims to improve the stability and accuracy of regression models by reducing their variance, leading to better performance on unseen data. Advantages of bagging regression mainly include variance reduction, improved robustness and simplicity. Scikit-learn[11] provides a

bagging regressor class that can be used with any base estimator. It simplifies the creation of bagged ensembles by allowing you to specify the number of estimators (n_estimators), the maximum fraction of the dataset to draw for each estimator (max_samples), and other parameters.

2. Random forest[12] is an ensemble learning technique that constructs multiple decision trees and outputs the mode of their predictions for classification tasks. This method often outperforms support vector machines (SVMs) and has proven successful in many classification challenges. Random Forest offers several advantages: it processes quickly, scales well with large datasets, exhibits robustness against noise, resists overfitting, and provides models that are easy to interpret and visualize. Moreover, it requires minimal parameter tuning, making it user-friendly. Scikit-learn[11] provides a random forest regressor class that can be used with any base estimator. If bootstrap = true (which is the default), the size of the sub-samples is controlled by the max_samples parameter; otherwise, the entire dataset is used to build each tree.

3. Gradient boosting regression[13] (GBR) is a powerful machine-learning algorithm used for both regression and classification tasks. It belongs to the family of boosting algorithms which combine weak learners into a strong learner in an iterative fashion. In the case of GBR, the weak learners are typically decision trees. Scikit-learn[11] provides a Gradient Boosting Regressor class that can be used with any base estimator. n_estimators parameter of GBR refers to the number of learning algorithms used by gradient boosting regression. Since each learning algorithm is a decision tree, the max_depth parameter determines the number of nodes in the tree. Selecting an appropriate number of nodes can lead to better data fitting, whereas too many nodes may result in overfitting. The loss parameter dictates the loss function and directly impacts the error measurement. The default value ls stands for least squares.

Experimental details

Materials Synthesis

Few-layer $MoSe_2$ was prepared by ultrasonication-assisted liquid-phase exfoliation of bulk $MoSe_2$. Specifically, 75.0 mg bulk $MoSe_2$ was dispersed in 30 mL of deionized water/isopropanol (DI-water/IPA, 60:40 v/v). The mixture was ultrasonicated at 450 W for 6 h in an ice bath. After standing for 8 h, the top 1/3 supernatant was collected for subsequent use.

CrNi/$MoSe_2$ was prepared by a two-step procedure involving chemical deposition with acid washing. Specifically, 3.0 mg $CrCl_3 \cdot 6H_2O$ and 3.0 mg $NiSO_4 \cdot 7H_2O$ was mixed with 15 mL of few-layer $MoSe_2$ dispersion. Under rapid stirring and ambient conditions, the mixed solution was added with 25.0 mg of $NaBH_4$ and then reacted for 1 h. Further, the result was washed with 15 mL of HCl (2.4 mol L^{-1}) for 1 h. Followed by DI-water washing and centrifugation, the obtained material is collected and labeled as CrNi/$MoSe_2$. Cr/$MoSe_2$ and Ni/$MoSe_2$ was also prepared by the synthesis method but only one of metal salts added.

Physical characterizations

Raman spectra were recorded on a Thermo Scientific DXR Raman microscope with a 532 nm laser. QUANTA 450 scanning electron microscope (SEM) was used to analyze the morphology and size of the samples, and the element content and element mapping map were obtained. XRD was performed on a Smart Lab SE Advanced Kα-Difftometer with Cu Kα radiation (λ = 1.5418 Å) at a current of 30 mA and a voltage of 40 kV. EXAFS was performed on Table XAFS-500 (Specreation Instruments Co., Ltd).

Electrochemical Characterization

A catalyst ink was prepared by ultrasonically dispersing 5.0 mg of the synthetic catalyst for 1 h in a mixture containing 750 μL isopropanol, 220 μL DI water, and 30 μL Nafion solution. The

catalyst ink was deposited onto a gas diffusion layer (GDL; effective catalytic area: 1 cm^2) at a loading of 0.5, 1.5 and 2.5 mg cm^{-2} and dried overnight under ambient conditions.

All electrochemical measurements were performed using a CHI 760E workstation in a flow-cell configuration with the synthesized catalyst as the working electrode, a Hg/Hg_2Cl_2 (saturated KCl) reference electrode, and a coated titanium anode (Dimensionally Stable Anode, DSA) counter electrode, separated by a Nafion 211 membrane (pre-treated sequentially: 5 wt% H_2O_2 at 80 °C for 3 h; DI-water at 80 °C for 1 h; 0.5 M H_2SO_4 at 80 °C for 2 h; 0.5 M H_2SO_4 at 100 °C for 8 h; DI-water at 80 °C for 1 h; final DI-water rinse). 0.1 M Na_2SO_4 electrolyte and 0.05 M H_2SO_4 absorption liquid flowed at 40 mL min^{-1}, with gas flow at 20 mL min^{-1}.

All measured potentials in this study were converted to the reversible hydrogen electrode (RHE) scale using the equation: $E_{RHE} = E_{Hg/Hg_2Cl_2} + 0.059 \times pH + 0.242$. Prior to electrochemical testing, all consumables—including working electrodes, reaction vessels, membranes, and electrolytes—were thoroughly cleaned. Nitrogen fixation activity was activated through cyclic voltammetry (CV) at 50 mV s^{-1} from -1.2 to 0 V (*vs.* RHE), followed by chronoamperometry at various potentials for 1 h under continuous N_2 bubbling.

Determination of NH_3 by Indophenol Blue Method

Following chronopotentiometry test, catholyte, anolyte, and twice absorption liquid was collected. The corresponding membrane was immersed in 50 mL of 0.05 M H_2SO_4 for 24 h. All solutions were analyzed to assess nitrogen fixation performance.

For preparation of chromogenic reagents, 2.0 mL of 1 M NaOH solution was dissolved in 5 wt% of sodium citrate and 5 wt% of salicylic acid as solution A, and 1.0 mL of 0.05 M NaClO solution and 0.2 mL 1 wt% of $C_5FeN_6Na_2O$ aqueous solution were label as B and C.

Then, 2.0 mL aliquots of the test solutions were sequentially mixed with chromogenic reagents A, B, and C. The mixture was incubated in darkness at ambient temperature for 2 h, followed by UV-Vis measurements across 550 ~ 750 nm. Ammonia concentration was determined spectrophotometrically by comparing absorption peaks at 655 nm between N_2-saturated systems.

Calculations for Faradic Efficiency (FE) and NH_3 Yield

The FE and NH_3 Yield are calculated as follows:

$$\mathrm{FE} = 3F \times c(\mathrm{NH_3}) \times \frac{V}{17 \times Q}$$

$$\mathrm{Yeild} = c(\mathrm{NH_3}) \times V / (t \times m)$$

Where F is Faradic constant, $c(\mathrm{NH_3})$ is NH_3 concentration, V is the volume of electrolyte, t is the reaction time and m is the catalyst mass.

Supplementary Figures

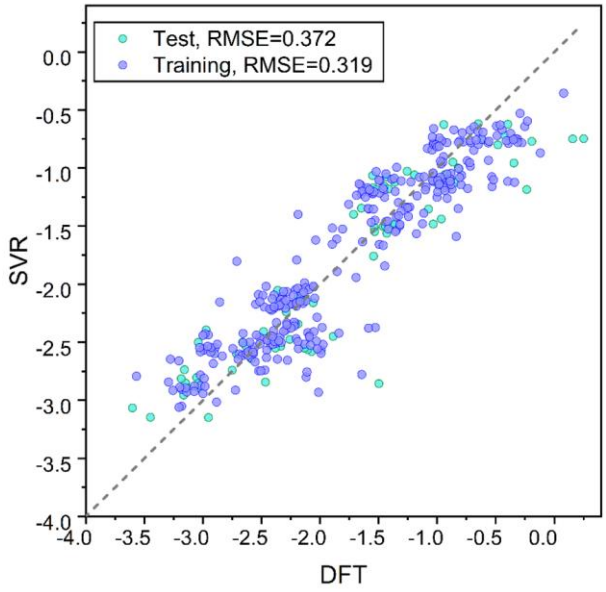

Figure S1 Prediction performance of SVR (Support Vector Regression, kernel='linear', epsilon=0.4) plot between DFT-Calculations and Machine Learning Outputs. The result of 100 random leave-n-out trials is the MAE value of 0.259, the RMSE value of 0.363 and the R^2 score of 0.839.

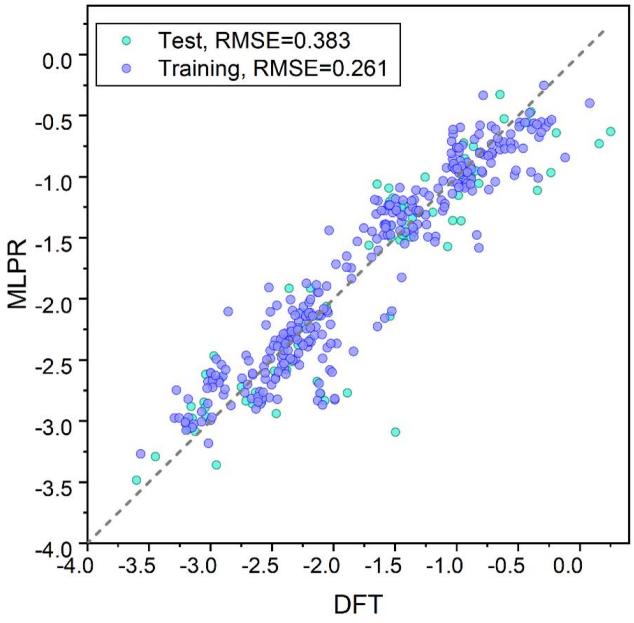

Figure S2 Prediction performance of MLPR (Multi-layer Perceptron Regressor, solver='lbfgs', alpha=0.0001, max-iter=10000) plot between DFT-Calculations and Machine Learning Outputs. The result of 100 random leave-n-out trials is the MAE value of 0.276, the RMSE value of 0.362 and the R^2 score of 0.802.

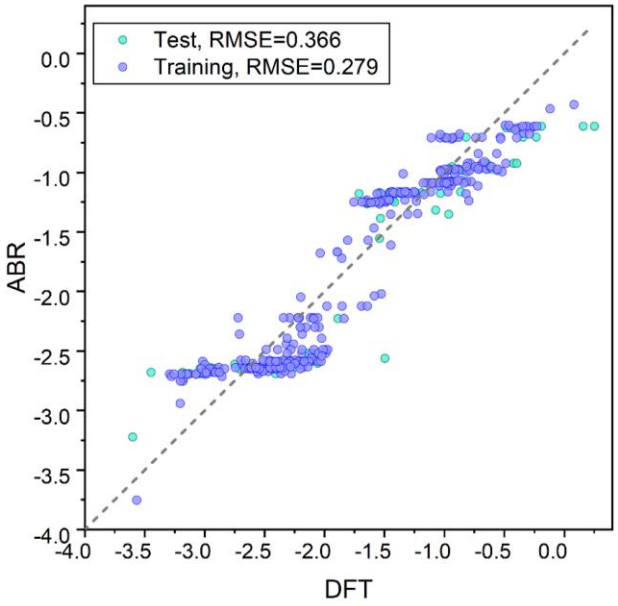

Figure S3 Prediction performance of ABR (Ada Boost Regressor) plot between DFT-Calculations and Machine Learning Outputs. The result of 100 random leave-n-out trials is the MAE value of 0.307, the RMSE value of 0.240 and the R^2 score of 0.872.

	RFR	GBR	LR	Bagging
MAE	0.135	0.116	0.248	0.139
RMSE	0.219	0.172	0.334	0.227
R^2	0.933	0.962	0.843	0.927

Figure S4 The table which shows MAE, RMSE, and R^2 of four ML models.

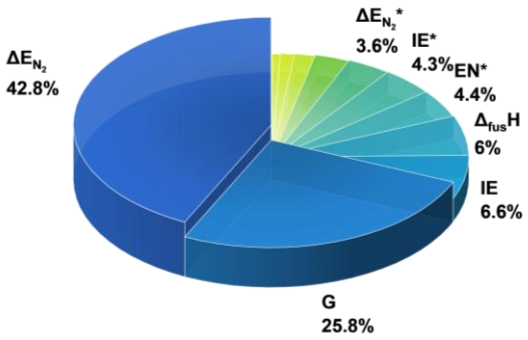

Figure S5 Feature importance heatmap for the GBR (importance data was normalized after removing out two features, N_N and N_H).

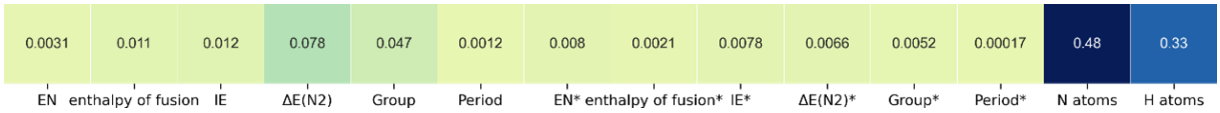

Figure S6 Feature importance heatmap for the GBR.

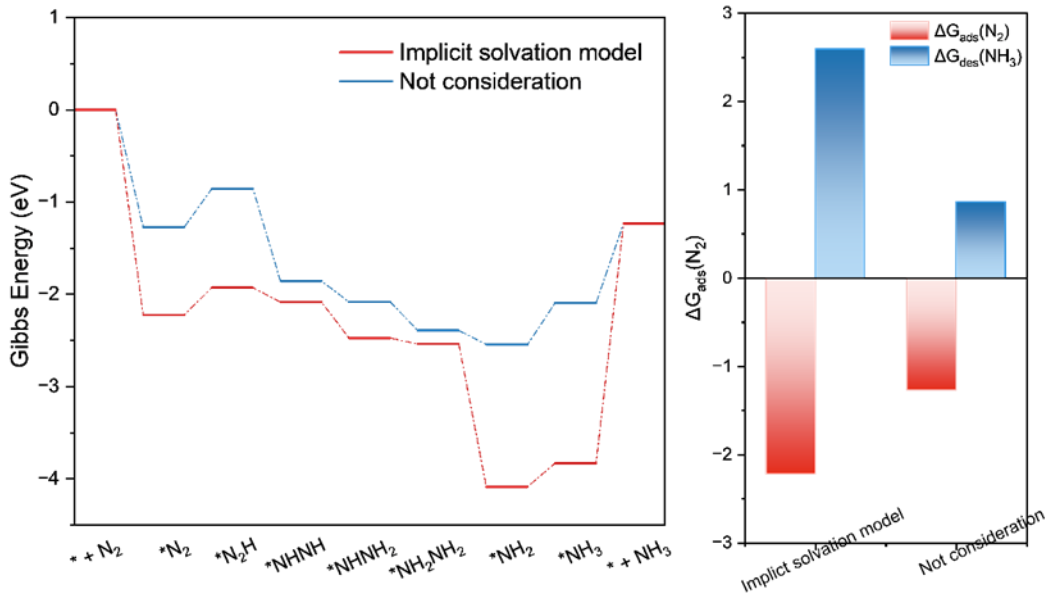

Figure S7 NRR energy diagrams for CrNi/$MoSe_2$ via enzymatic mechanism with and without implicit solvation model (left); the bar graph of N_2 adsorption energy and NH_3 desorption energy with and without implicit solvation model (right**).**

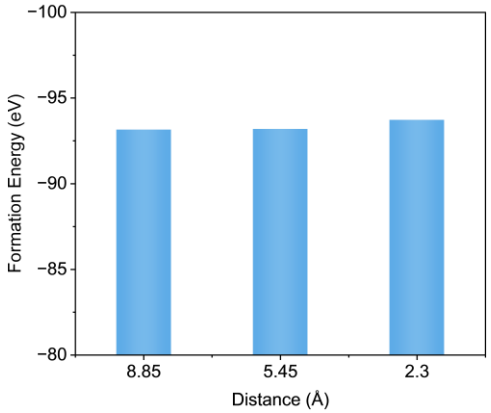

Figure S8 The formation energies of next-next-nearest neighbor (~ 8.85 Å), next-nearest neighbor (~ 5.45 Å) to nearest neighbor (~ 2.30 Å).

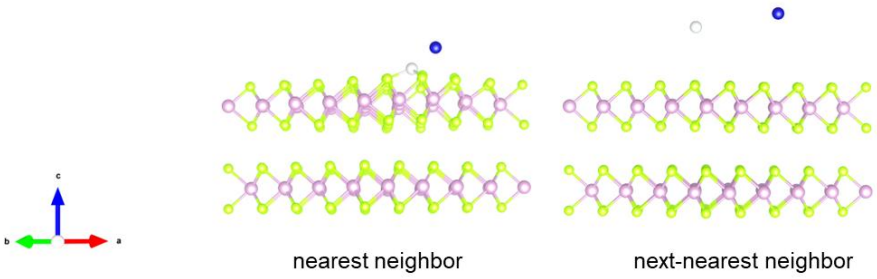

Figure S9 Configurations of nearest neighbor and next-nearest neighbor after structural optimization. (green balls, light rose balls, blue balls, grey balls and purple balls represent of Mo, Se, Cr, Ni, and N atoms).

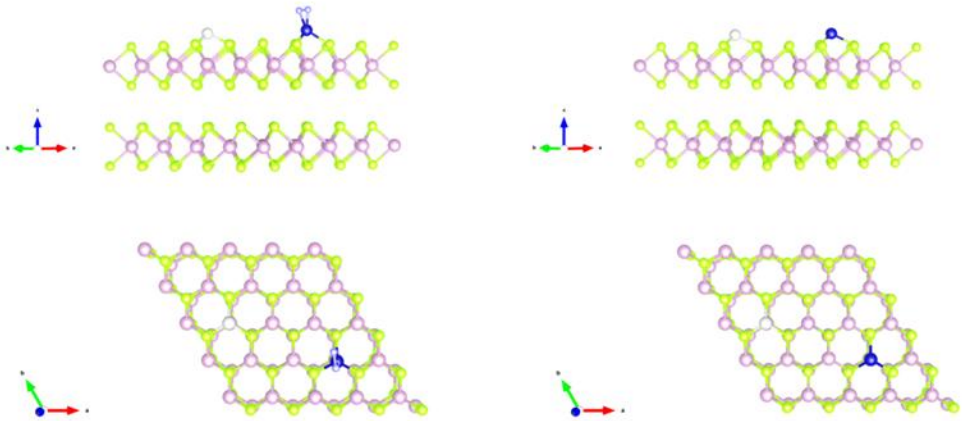

Figure S10 next-next-nearest neighbor (right) and relevant *N_2 (left) configurations after structural optimization. (green balls, light rose balls, blue balls, grey balls and purple balls represent of Mo, Se, Cr, Ni, and N atoms).

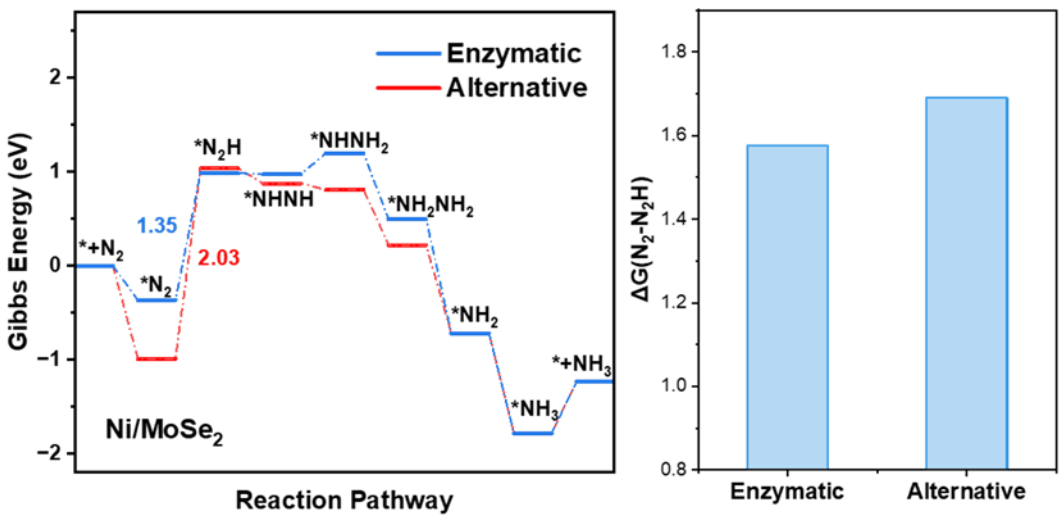

Figure S11 Free energy diagrams in NRR via enzymatic and alternative mechanisms in Ni sites of $Ni/MoSe_2$ (Left); $\Delta G(N_2\text{-}N_2H)$ comparison in Ni sites of $CrNi/MoSe_2$ via enzymatic and alternative mechanisms (Right).

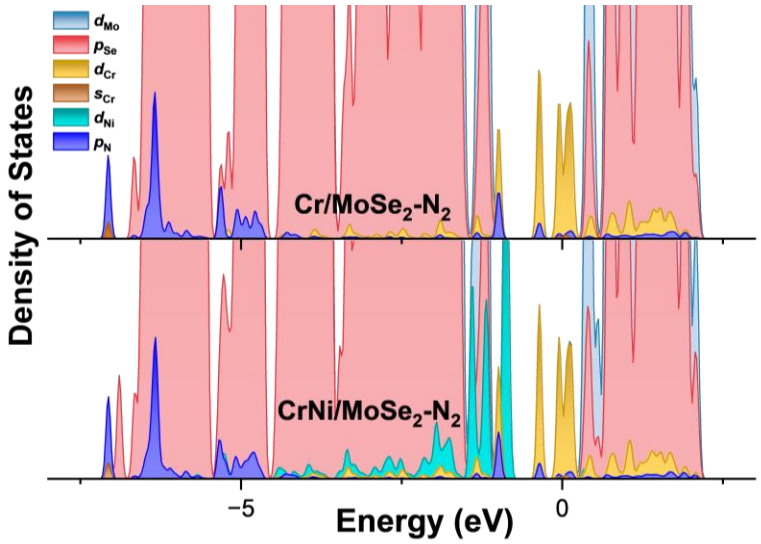

Figure S12 Simulated density of states (DOS) profiles of CrNi/$MoSe_2$-N_2 and Cr/$MoSe_2$-N_2.

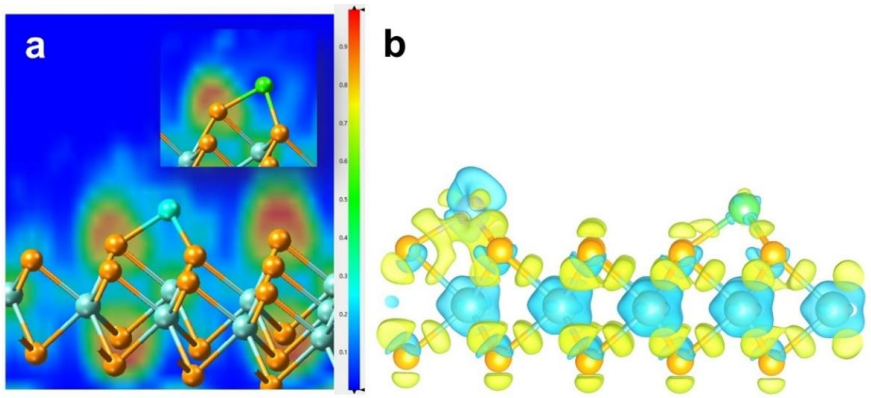

Figure S13 (a) Calculated electron location function (ELF) and (b) charge difference of CrNi/$MoSe_2$. Yellow, blue, aqua and green balls represent Se, Mo, Cr and Ni atoms; Green and blue regions represent electron accumulation and electron depletion, respectively.

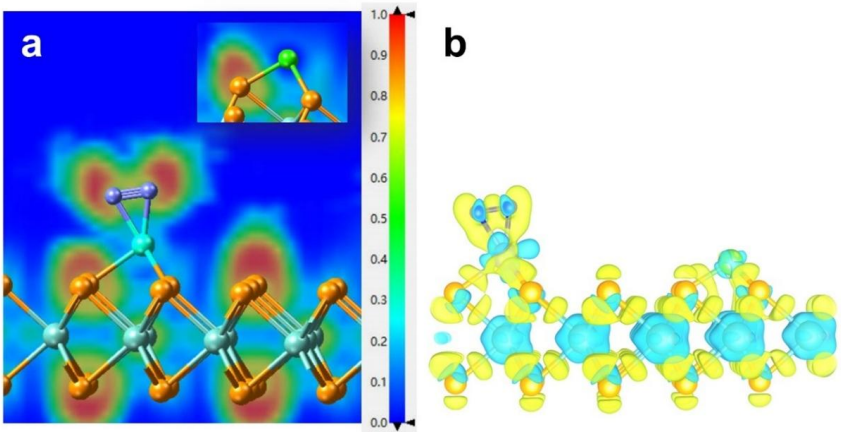

Figure S14 (a) Calculated electron location function (ELF) and (b) charge difference of $CrNi/MoSe_2$-N_2. Yellow, blue, aqua and green balls represent Se, Mo, Cr and Ni atoms; Green and blue regions represent electron accumulation and electron depletion, respectively.

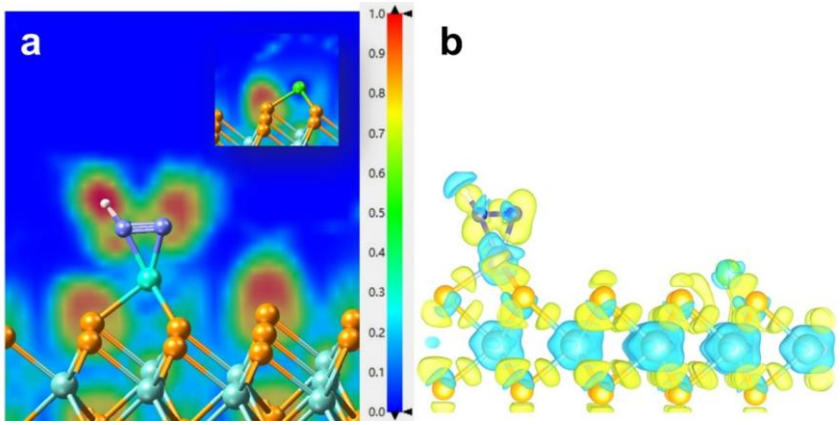

Figure S15 (a) Calculated electron location function (ELF) and (b) charge difference of CrNi/$MoSe_2$-N_2H. Yellow, blue, aqua and green, white balls represent Se, Mo, Cr and Ni, H atoms; Green and blue regions represent electron accumulation and electron depletion, respectively.

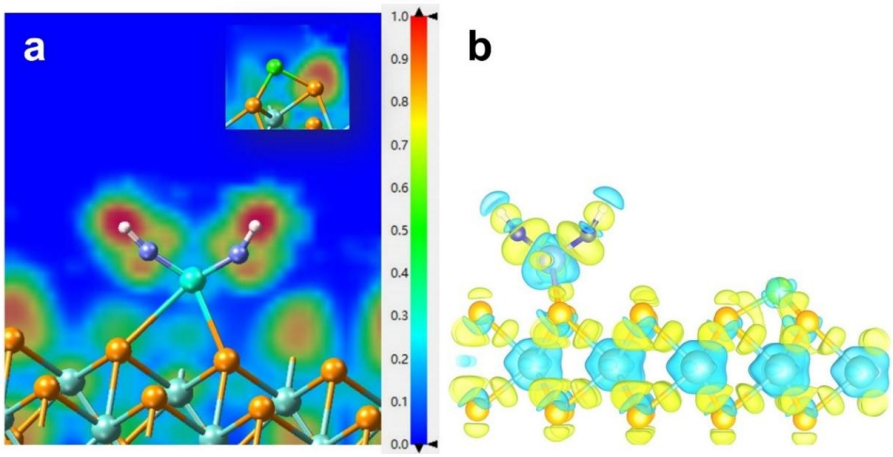

Figure S16 (a) Calculated electron location function (ELF) and (b) charge difference of $CrNi/MoSe_2$-N_2H_2. Yellow, blue, aqua and green, white balls represent Se, Mo, Cr and Ni, H atoms; Green and blue regions represent electron accumulation and electron depletion, respectively.

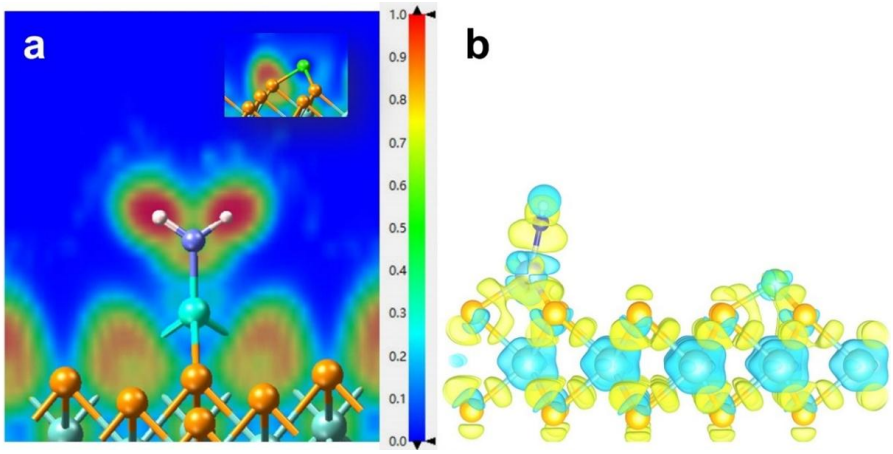

Figure S17 (a) Calculated electron location function (ELF) and (b) charge difference of $CrNi/MoSe_2$-NH_2. Yellow, blue, aqua and green, white balls represent Se, Mo, Cr and Ni, H atoms; Green and blue regions represent electron accumulation and electron depletion, respectively.

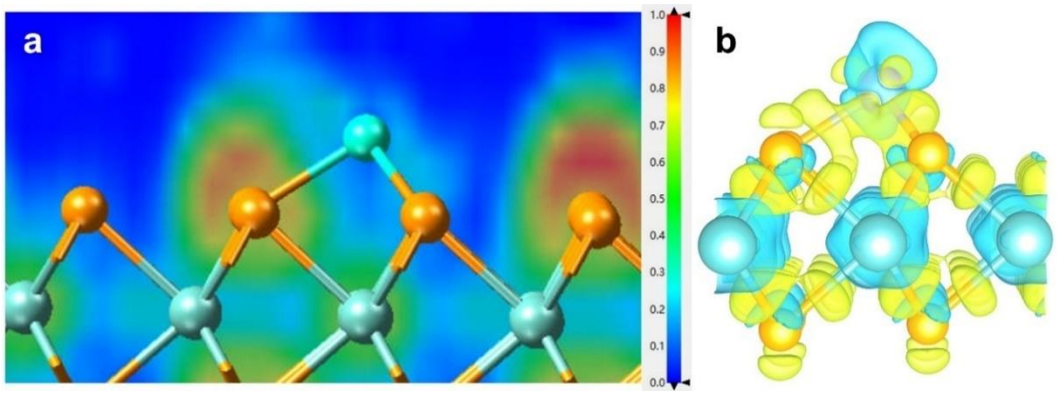

Figure S18 (a) Calculated electron location function (ELF) and (b) charge difference of Cr/$MoSe_2$. Yellow, blue and aqua balls represent Se, Mo and Cr atoms; Green and blue regions represent electron accumulation and electron depletion, respectively.

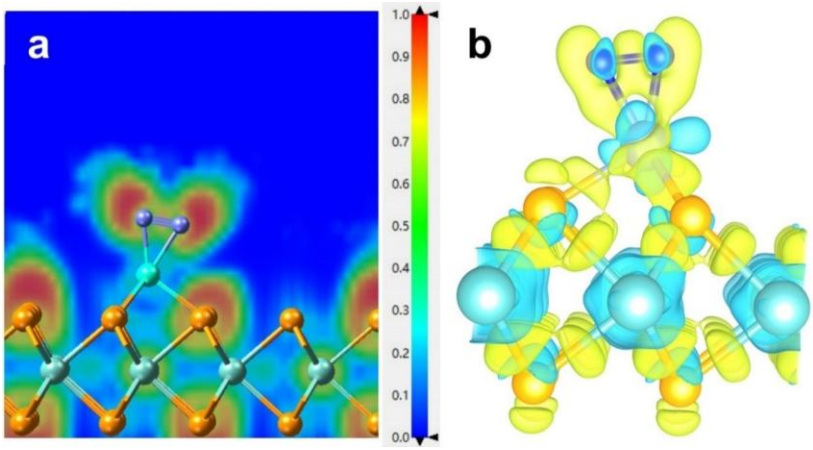

Figure S19 (a) Calculated electron location function (ELF) and (b) charge difference of Cr/$MoSe_2$-N_2. Yellow, blue and aqua balls represent Se, Mo and Cr atoms; Green and blue regions represent electron accumulation and electron depletion, respectively.

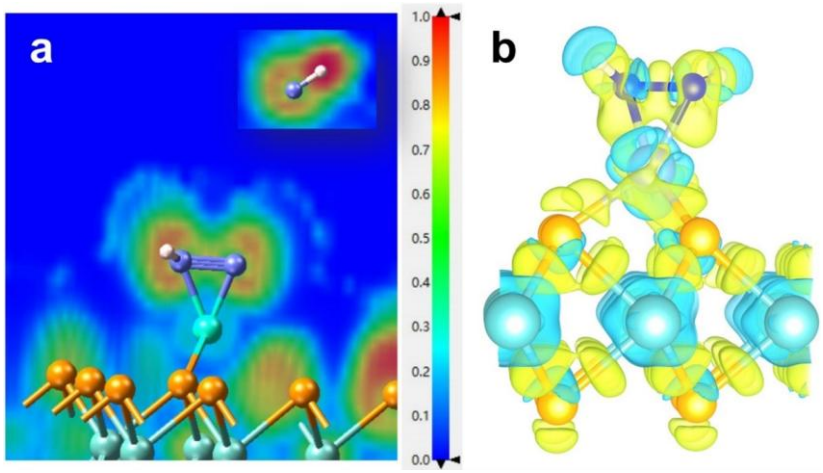

Figure S20 (a) Calculated electron location function (ELF) and (b) charge difference of Cr/$MoSe_2$-N_2H_2. Yellow, blue and aqua, while balls represent Se, Mo and Cr, H atoms; Green and blue regions represent electron accumulation and electron depletion, respectively.

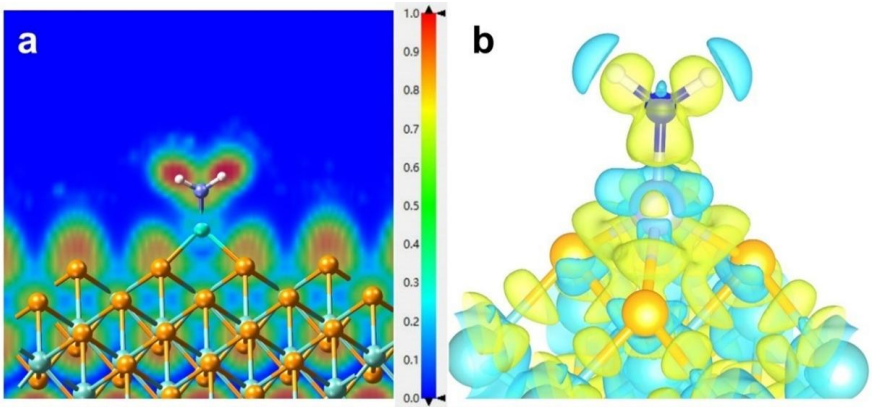

Figure S21 (a) Calculated electron location function (ELF) and (b) charge difference of Cr/$MoSe_2$-NH_2. Yellow, blue and aqua, white balls represent Se, Mo and Cr, H atoms; Green and blue regions represent electron accumulation and electron depletion, respectively.

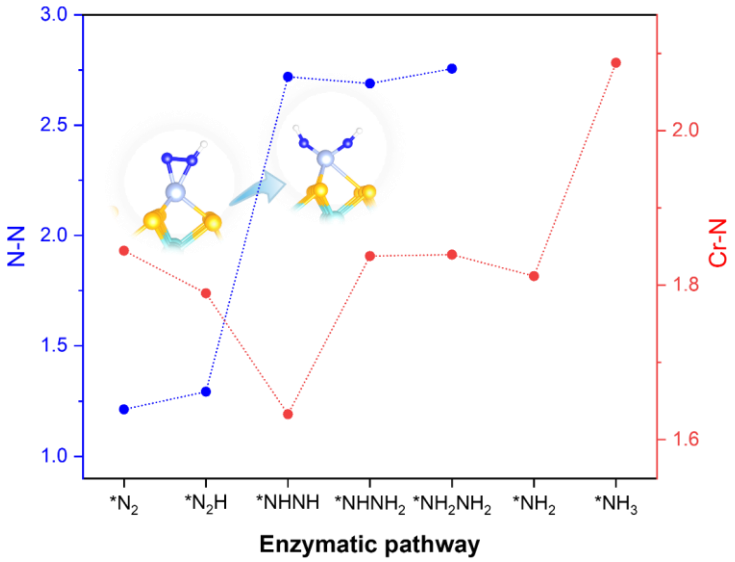

Figure S22 N-N and Cr-N bond length of intermediates for CrNi/$MoSe_2$ via enzymatic mechanism. The bond distance during the hydrogenation step of *N_2H to *NHNH indicates a sharp increase in N-N bond length and according decrease in Cr-N bond length. Immediately after, The Cr-N bond distance indicates gradual increase during the reduction steps of *NHNH to *NH_2.

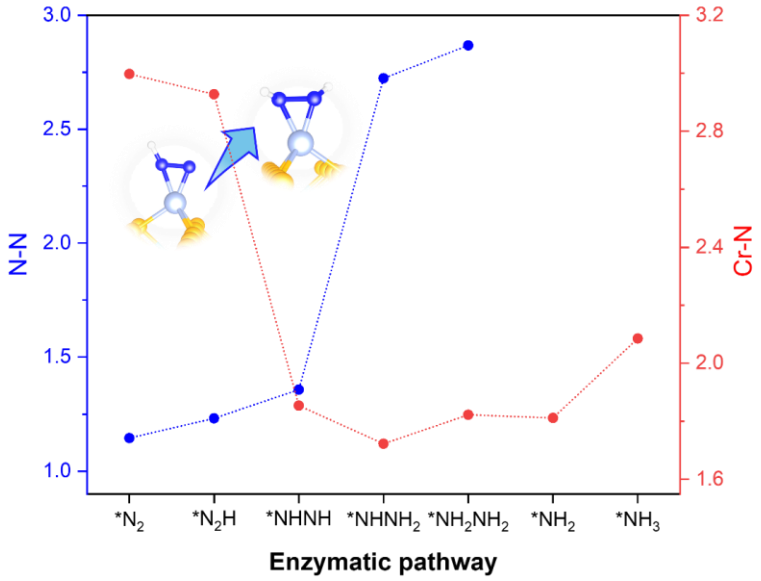

Figure S23 N-N and Cr-N bond length of intermediates for Cr/$MoSe_2$ via enzymatic mechanism.

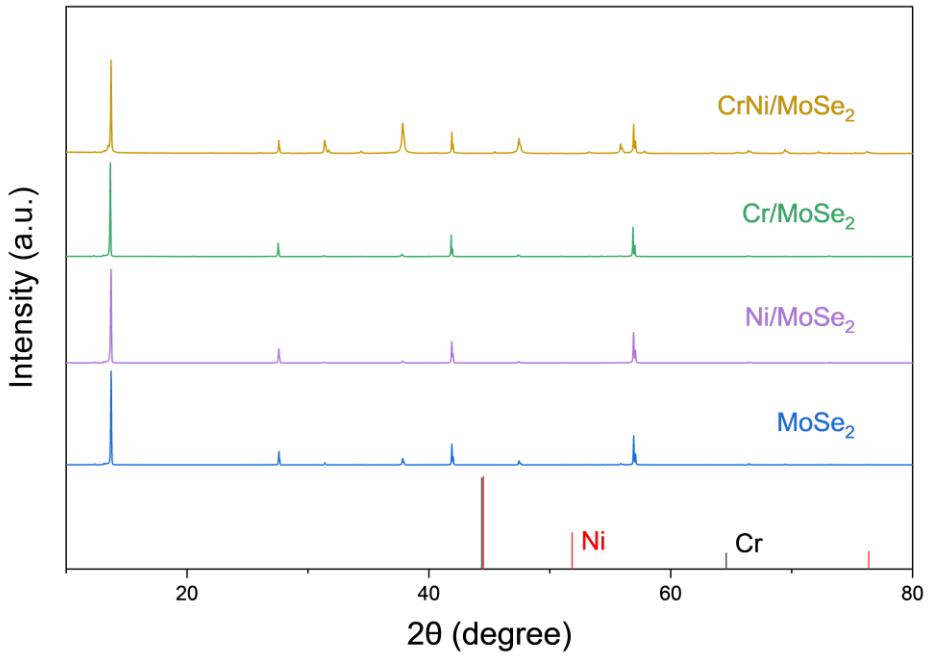

Figure S24 XRD spectra of $CrNi/MoSe_2$, $Cr/MoSe_2$, $Ni/MoSe_2$, $MoSe_2$ and the Ni and Cr standard.

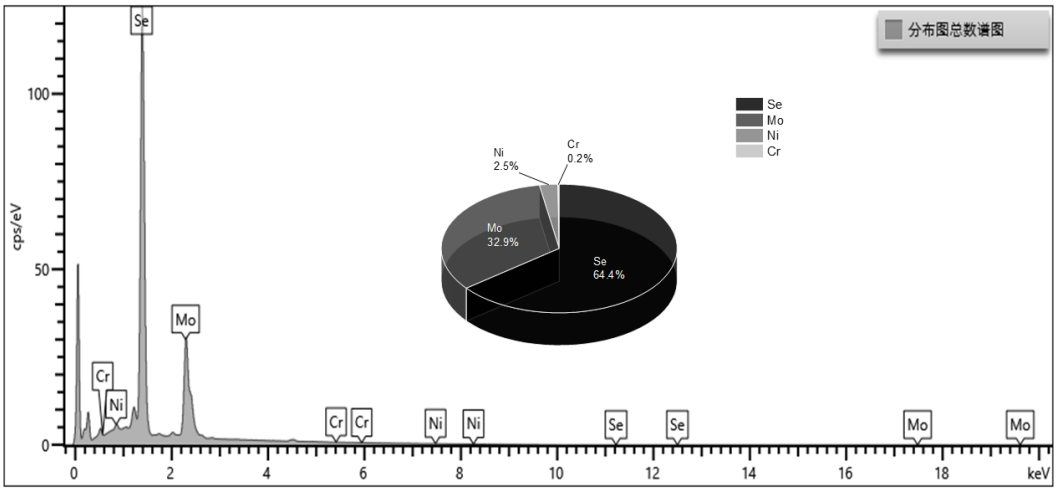

Figure S25 SEM-EDS spectra of CrNi/$MoSe_2$ and atomic ratio of Ni, Cr, Mo and Se (the inset).

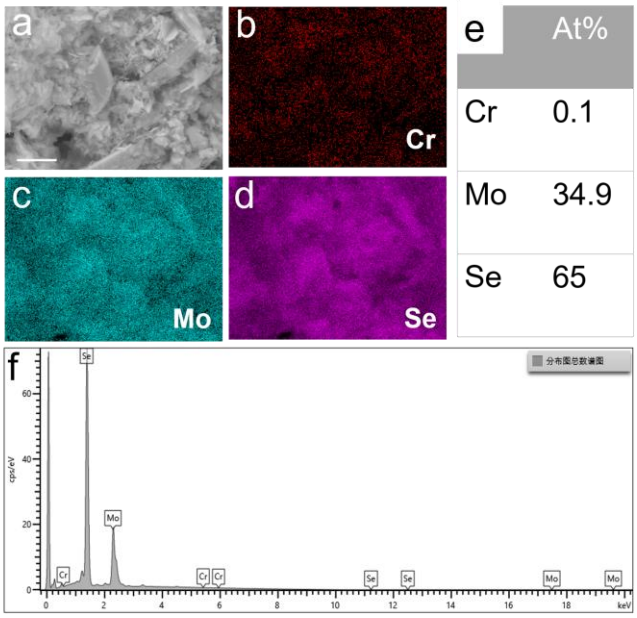

Figure S26 Morphological characterization of Cr/$MoSe_2$ nanosheets. (a) SEM image (scale bar, 2 μm); (b-d) SEM element mappings of Cr, Mo and Se; (e) Atomic ratio of Cr, Mo and Se; (f) SEM EDS spectra.

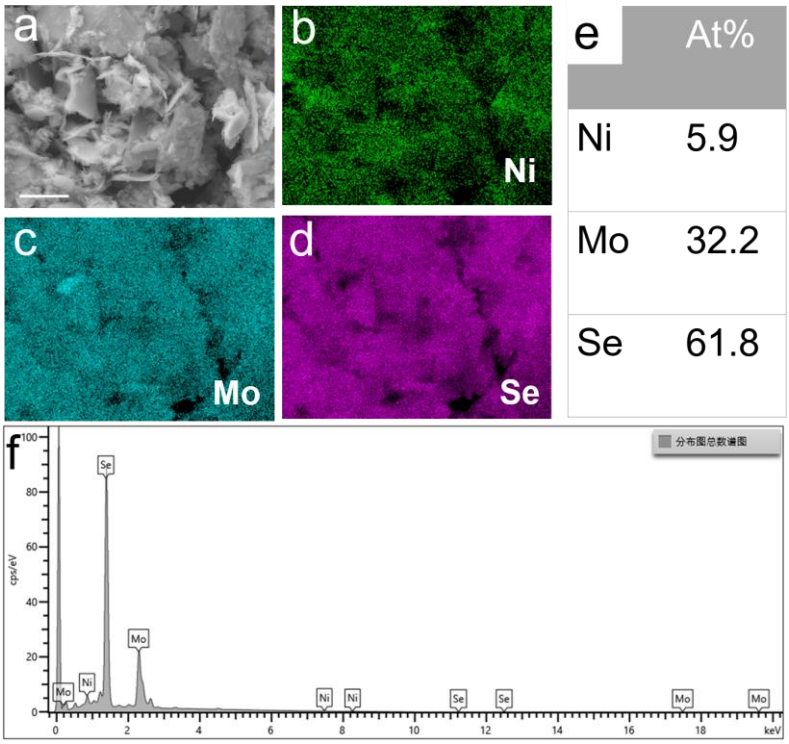

Figure S27 Morphological characterization of Ni/$MoSe_2$ nanosheets. (a) SEM image (scale bar, 2 μm); (b-d) SEM element mappings of Ni, Mo and Se; (e) Atomic ratio of Ni, Mo and Se; (f) SEM EDS spectra.

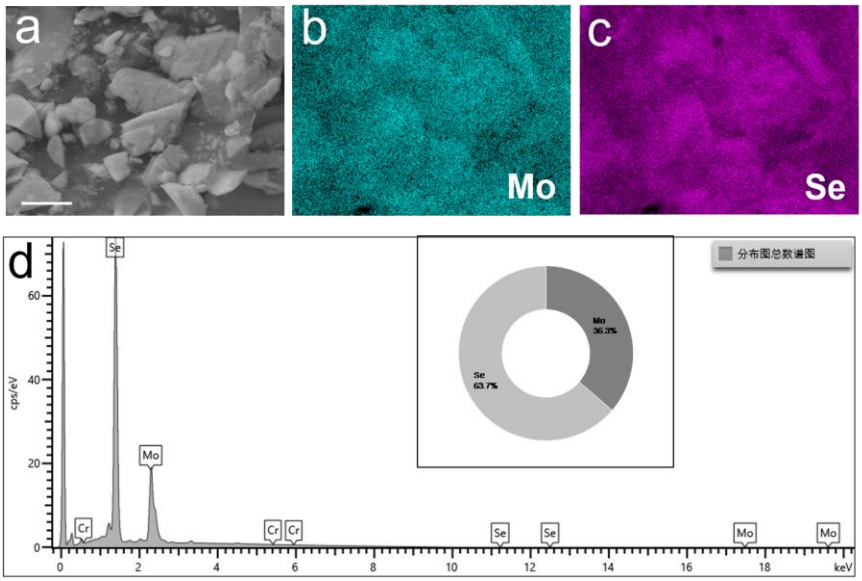

Figure S28 Morphological characterization of $MoSe_2$ nanosheets. (a) SEM image (scale bar, 2 μm); (b, c) SEM element mappings of Mo and Se; (d) SEM EDS spectra and atomic ratio of Mo and Se (the inset).

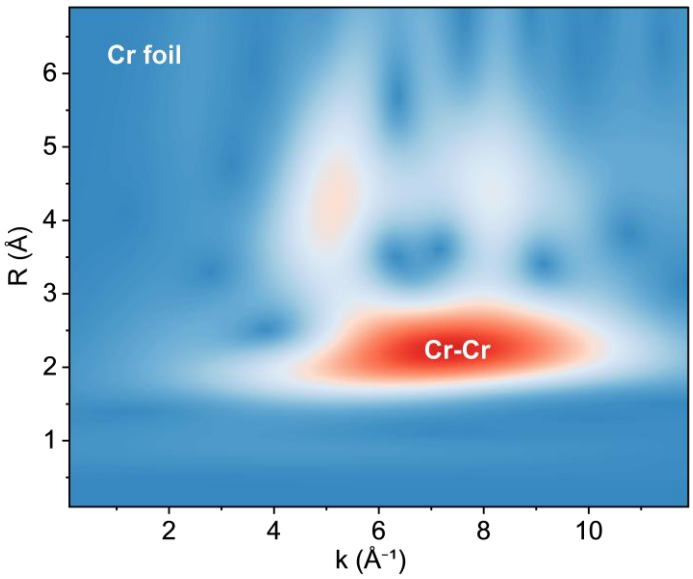

Figure S29 Wavelet transform (WT)-EXAFS contour plots providing two-dimensional resolution of the Cr–Cr scattering paths in Cr foil.

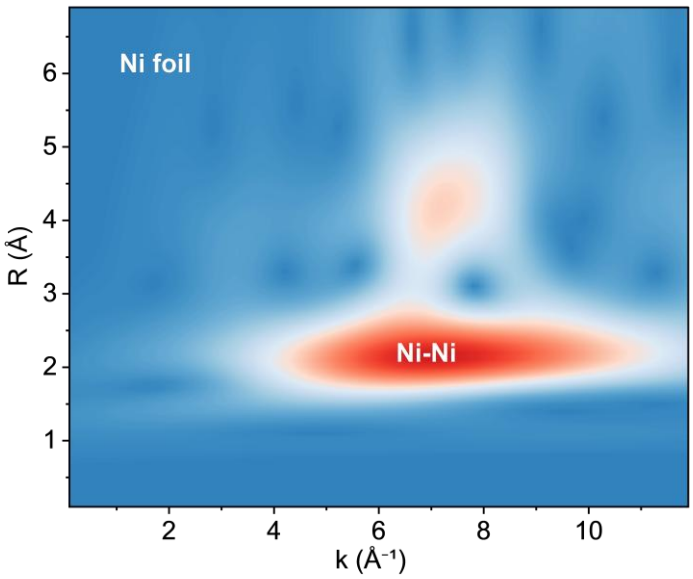

Figure S30 Wavelet transform (WT)-EXAFS contour plots providing two-dimensional resolution of the Ni–Ni scattering paths in Ni foil.

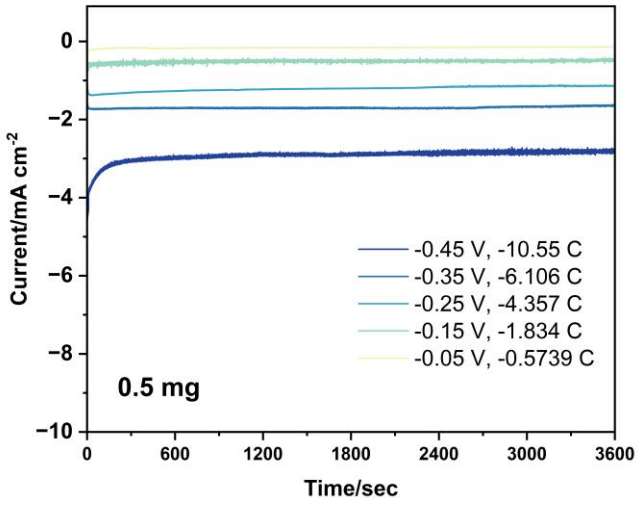

Figure S31 Chronoamperometry curves of CrNi/$MoSe_2$ with loading mass of 0.5 mg cm^{-2} at −0.05 ~ −0.45 V (*vs.* RHE).

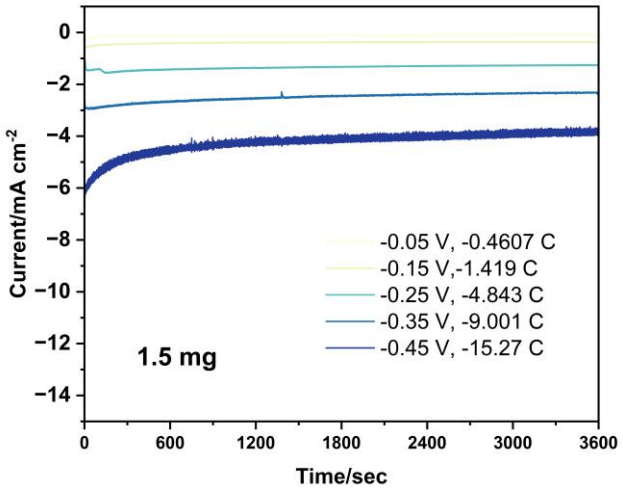

Figure S32 Chronoamperometry curves of CrNi/$MoSe_2$ with loading mass of 1.5 mg cm^{-2} at −0.05 ~ −0.45 V (*vs.* RHE).

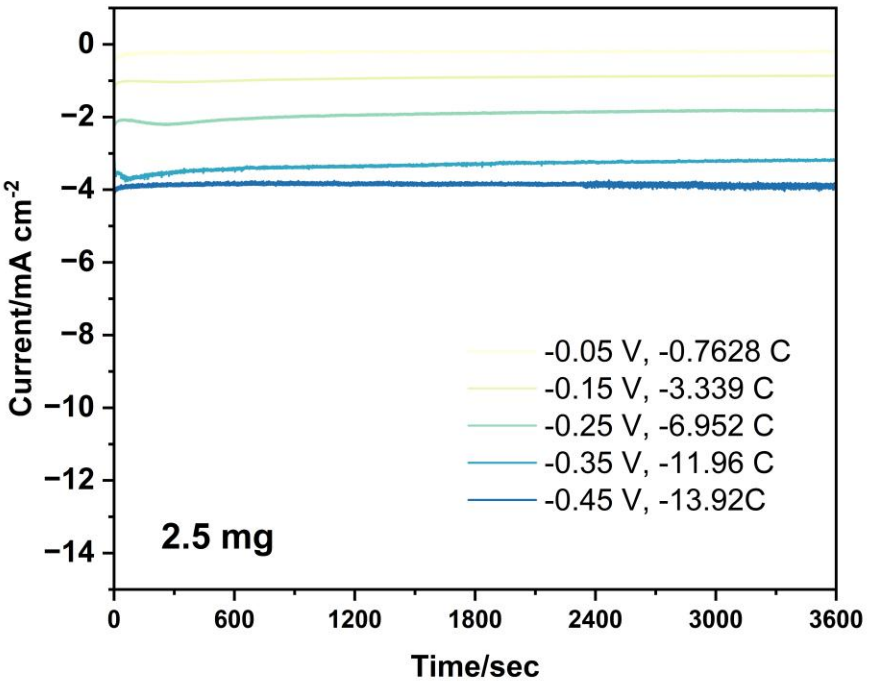

Figure S33 Chronoamperometry curves of CrNi/$MoSe_2$ with loading mass of 2.5 mg cm^{-2} at −0.05 ~ −0.45 V (*vs.* RHE).

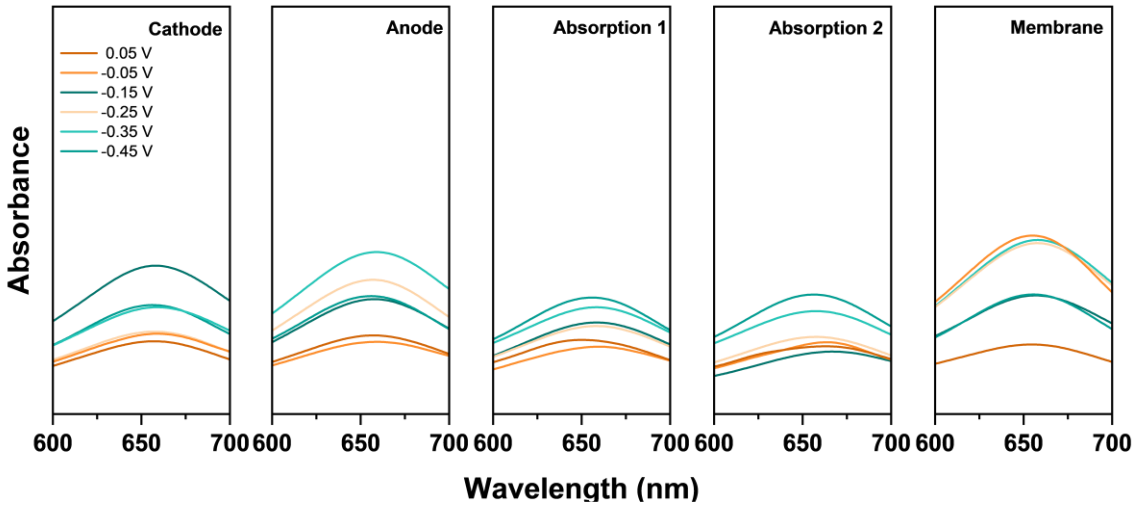

Figure S34 UV-vis absorption spectrum of CrNi/$MoSe_2$ (loading mass: 0.5 mg cm^{-2}) electrode after potentiostatic tests at different potentials in N_2-saturated 0.1 M Na_2SO_4 solutions.

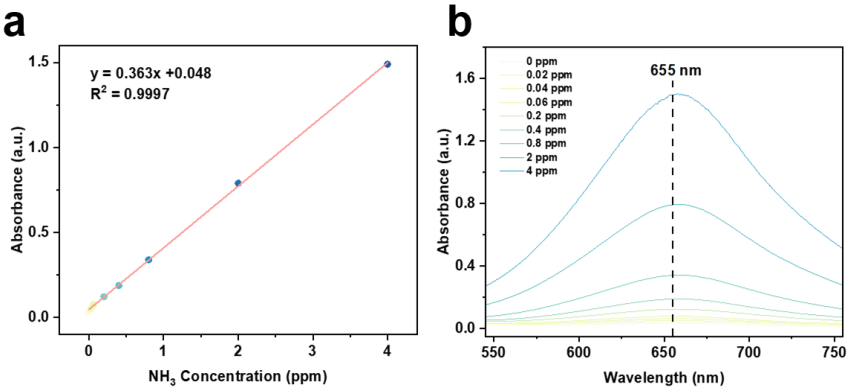

Figure S35 Calibration curve for NH_3 using a known concentration of NH_4Cl solution in 0.1 M Na_2SO_4 solution. (a) UV-vis absorption spectra of indophenol assays with different NH_3 concentrations after incubated for 2 h; (b) Calibration curve used for estimation of NH_3 concentrations.

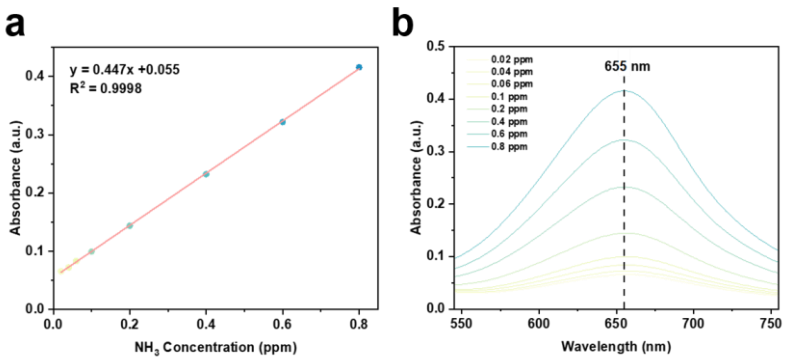

Figure S36 Calibration curve for NH_3 using a known concentration of NH_4Cl solution in 0.05 M H_2SO_4 solution. (a) UV-vis absorption spectra of indophenol assays with different NH_3 concentrations after incubated for 2 h; (b) Calibration curve used for estimation of NH_3 concentrations.

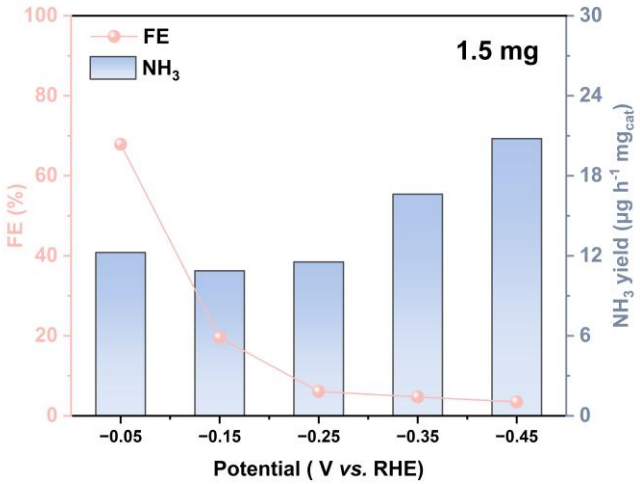

Figure S37 NH_3 yields and FEs of CrNi/$MoSe_2$ with loading mass of 1.5 mg cm^{-2} at different applied potentials.

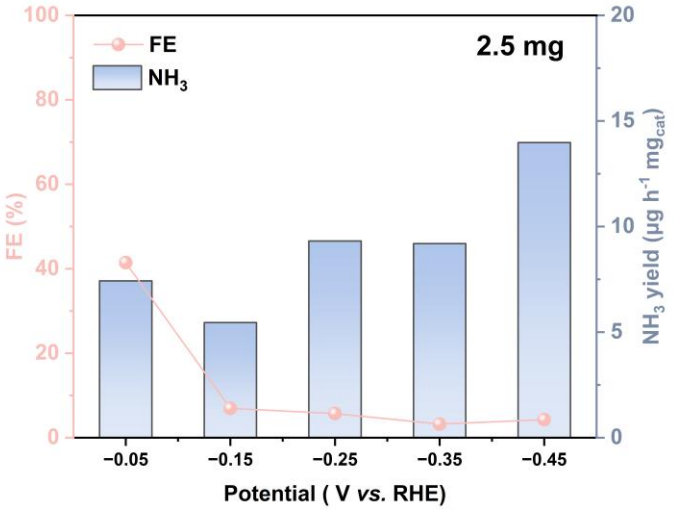

Figure S38 NH_3 yields and FEs of CrNi/$MoSe_2$ with loading mass of 2.5 mg cm^{-2} at different applied potentials.

Supplementary Tables

Table S1 Adsorption energy calculated through DFT and machine learning by GBR model for the data set.

Catalyst	Adsorption Species	DFT/eV	GBR/eV	Type of data
CoFe/MoSe$_2$	*N_2H	-0.292	-0.319	training
CoRh/MoSe$_2$	*NH_2	-1.527	-1.588	training
CoSc/MoSe$_2$	*NH_2	-1.586	-1.620	training
CrFe/MoSe$_2$	*NH_2	-2.912	-2.930	training
FeAg/MoSe$_2$	*N_2H	-0.651	-0.689	training
FeAg/MoSe$_2$	*NH_3	-2.156	-2.155	training
FeAg/MoSe$_2$	*N_2	-1.367	-1.337	training
FeCd/MoSe$_2$	*NH_3	-2.210	-2.147	training
FeCd/MoSe$_2$	*NH_2	-2.091	-2.094	training
FeCd/MoSe$_2$	*N_2	-1.194	-1.284	test
FeCo/MoSe$_2$	*NH_2	-2.090	-2.107	training
FeCo/MoSe$_2$	*N_2H	-0.686	-0.665	training
FeCo/MoSe$_2$	*N_2	-1.438	-1.319	training
FeCr/MoSe$_2$	*NH_2	-2.105	-2.091	training
FeCr/MoSe$_2$	*N_2H	-0.649	-0.695	test
FeCu/MoSe$_2$	*NH_2	-1.839	-1.989	training
FeCu/MoSe$_2$	*NH_3	-2.057	-2.049	training
FeCu/MoSe$_2$	*N_2	-1.257	-1.163	test
FeCu/MoSe$_2$	*N_2H	-0.398	-0.539	test
FeHf/MoSe$_2$	*NH_2	-1.992	-2.089	training
FeHf/MoSe$_2$	*NH_3	-2.202	-2.093	training
FeHf/MoSe$_2$	*N_2H	-0.649	-0.694	training
FeHf/MoSe$_2$	*N_2	-1.359	-1.343	training
FeIr/MoSe$_2$	*NH_3	-2.313	-2.215	training
FeIr/MoSe$_2$	*N_2H	-0.720	-0.734	training
FeIr/MoSe$_2$	*NH_2	-2.106	-2.203	test
FeIr/MoSe$_2$	*N_2	-1.546	-1.387	test
FeMn/MoSe$_2$	*N_2H	-0.786	-0.688	training
FeMn/MoSe$_2$	*NH_2	-2.190	-2.083	training
FeMo/MoSe$_2$	*N_2H	-0.609	-0.709	training
FeMo/MoSe$_2$	*N_2	-1.386	-1.358	training
FeMo/MoSe$_2$	*NH_2	-2.030	-2.082	training
FeNb/MoSe$_2$	*NH_3	-2.046	-2.066	training
FeOs/MoSe$_2$	*N_2H	-0.713	-0.744	training
FeOs/MoSe$_2$	*NH_3	-2.260	-2.220	training
FeOs/MoSe$_2$	*N_2	-1.455	-1.397	training
FeOs/MoSe$_2$	*NH_2	-2.072	-2.197	test

FePt/$MoSe_2$	*NH_2	-1.991	-2.088	training
FePt/$MoSe_2$	*NH_3	-2.204	-2.133	training
FePt/$MoSe_2$	*N_2H	-0.558	-0.643	training
FeRh/$MoSe_2$	*N_2H	-0.620	-0.685	training
FeRh/$MoSe_2$	*N_2	-1.450	-1.334	test
FeRh/$MoSe_2$	*NH_2	-2.135	-2.110	test
FeRu/$MoSe_2$	*NH_3	-2.321	-2.208	training
FeRu/$MoSe_2$	*NH_2	-2.131	-2.196	training
FeRu/$MoSe_2$	*N_2	-1.363	-1.398	test
FeSc/$MoSe_2$	*NH_2	-2.023	-2.098	training
FeSc/$MoSe_2$	*N_2H	-0.615	-0.720	test
FeTi/$MoSe_2$	*N_2H	-0.490	-0.611	training
FeTi/$MoSe_2$	*NH_2	-1.975	-2.023	training
FeTi/$MoSe_2$	*N_2H	-0.424	-0.611	test
FeV/$MoSe_2$	*NH_2	-2.053	-2.090	training
FeY/$MoSe_2$	*N_2	-1.331	-1.363	training
FeY/$MoSe_2$	*NH_3	-2.026	-2.068	training
FeZn/$MoSe_2$	*NH_3	-2.095	-2.129	training
FeZn/$MoSe_2$	*NH_2	-1.890	-2.086	test
HfSc/$MoSe_2$	*N_2H	-1.346	-1.181	training
HfSc/$MoSe_2$	*N_2	-1.714	-1.619	test
HfTi/$MoSe_2$	*NH_3	-2.285	-2.359	training
HfTi/$MoSe_2$	*N_2H	-0.345	-0.762	test
HfV/$MoSe_2$	*N_2H	-0.688	-0.886	training
HfV/$MoSe_2$	*NH_2	-3.278	-3.095	training
IrCo/$MoSe_2$	*NH_2	-2.118	-2.195	training
IrCo/$MoSe_2$	*NH_3	-2.291	-2.208	training
IrCu/$MoSe_2$	*NH_3	-1.982	-1.957	training
IrCu/$MoSe_2$	*NH_2	-1.644	-1.837	training
IrFe/$MoSe_2$	*N_2H	-0.791	-0.885	training
IrFe/$MoSe_2$	*N_2	-1.563	-1.522	training
IrFe/$MoSe_2$	*NH_3	-2.344	-2.371	training
IrNi/$MoSe_2$	*NH_3	-2.222	-2.166	training
IrNi/$MoSe_2$	*N_2	-1.268	-1.272	training
IrNi/$MoSe_2$	*N_2H	-0.563	-0.640	training
IrRu/$MoSe_2$	*NH_2	-3.017	-2.817	training
IrSc/$MoSe_2$	*NH_2	-2.722	-2.509	training
IrSc/$MoSe_2$	*N_2H	-0.890	-0.954	training
IrTi/$MoSe_2$	*N_2	-1.033	-1.306	test
IrV/$MoSe_2$	*NH_3	-2.220	-2.287	training
IrV/$MoSe_2$	*N_2	-1.307	-1.386	training
LaTi/$MoSe_2$	*N_2	-0.120	-0.157	training
LaV/$MoSe_2$	*NH_2	-2.857	-2.945	training
LaV/$MoSe_2$	*N_2H	0.079	0.068	training
MnAg/$MoSe_2$	*N_2	-1.667	-1.618	training
MnAg/$MoSe_2$	*N_2H	-1.043	-1.014	training

MnAg/$MoSe_2$	*NH_3	-2.409	-2.394	training
MnAg/$MoSe_2$	*NH_2	-2.635	-2.720	test
MnAu/$MoSe_2$	*N_2	-1.756	-1.680	training
MnCd/$MoSe_2$	*N_2	-1.489	-1.530	training
MnCd/$MoSe_2$	*NH_3	-2.487	-2.356	training
MnCd/$MoSe_2$	*NH_2	-2.662	-2.662	test
MnCu/$MoSe_2$	*NH_2	-2.474	-2.555	training
MnCu/$MoSe_2$	*N_2H	-0.857	-0.832	training
MnCu/$MoSe_2$	*NH_3	-2.282	-2.256	training
MnCu/$MoSe_2$	*N_2	-1.434	-1.412	test
MnFe/$MoSe_2$	*NH_2	-2.745	-2.685	training
MnFe/$MoSe_2$	*NH_3	-2.514	-2.359	training
MnHf/$MoSe_2$	*N_2H	-1.045	-0.964	training
MnHf/$MoSe_2$	*N_2	-1.613	-1.568	training
MnHf/$MoSe_2$	*NH_3	-2.289	-2.300	test
MnHf/$MoSe_2$	*NH_2	-2.585	-2.631	test
MnIr/$MoSe_2$	*N_2	-1.557	-1.584	training
MnIr/$MoSe_2$	*NH_3	-2.296	-2.371	training
MnIr/$MoSe_2$	*NH_2	-2.615	-2.697	training
MnIr/$MoSe_2$	*N_2H	-0.984	-0.980	training
MnLa/$MoSe_2$	*NH_2	-2.523	-2.631	training
MnLa/$MoSe_2$	*N_2	-1.544	-1.579	training
MnLa/$MoSe_2$	*NH_3	-2.188	-2.299	test
MnLa/$MoSe_2$	*N_2H	-0.866	-0.977	test
MnMo/$MoSe_2$	*NH_3	-2.334	-2.265	training
MnMo/$MoSe_2$	*N_2	-1.654	-1.538	training
MnMo/$MoSe_2$	*NH_2	-2.557	-2.555	training
MnMo/$MoSe_2$	*N_2H	-0.982	-0.934	training
MnNb/$MoSe_2$	*NH_3	-2.196	-2.271	training
MnNb/$MoSe_2$	*N_2H	-0.779	-0.929	training
MnNb/$MoSe_2$	*N_2	-1.416	-1.533	test
MnNi/$MoSe_2$	*NH_2	-2.657	-2.612	training
MnNi/$MoSe_2$	*N_2	-1.521	-1.502	training
MnNi/$MoSe_2$	*NH_3	-2.461	-2.293	training
MnNi/$MoSe_2$	*N_2H	-0.944	-0.898	test
MnOs/$MoSe_2$	*NH_2	-2.594	-2.689	training
MnOs/$MoSe_2$	*N_2H	-1.084	-0.987	training
MnOs/$MoSe_2$	*NH_3	-2.416	-2.374	training
MnOs/$MoSe_2$	*N_2	-1.688	-1.592	training
MnPd/$MoSe_2$	*NH_3	-2.475	-2.420	training
MnPd/$MoSe_2$	*N_2	-1.578	-1.624	training
MnPd/$MoSe_2$	*N_2H	-1.026	-1.020	training
MnPd/$MoSe_2$	*NH_2	-2.713	-2.746	test
MnPt/$MoSe_2$	*NH_3	-2.397	-2.367	training
MnPt/$MoSe_2$	*N_2	-1.549	-1.579	training
MnPt/$MoSe_2$	*NH_2	-2.666	-2.692	training

MnPt/$MoSe_2$	*N_2H	-1.001	-0.975	training
MnRe/$MoSe_2$	*NH_3	-2.247	-2.274	training
MnRe/$MoSe_2$	*N_2H	-0.819	-0.936	training
MnRe/$MoSe_2$	*N_2	-1.519	-1.540	test
MnRh/$MoSe_2$	*NH_2	-2.631	-2.659	training
MnRh/$MoSe_2$	*N_2	-1.539	-1.566	training
MnRh/$MoSe_2$	*N_2H	-1.011	-0.961	training
MnRh/$MoSe_2$	*NH_3	-2.392	-2.333	training
MnRu/$MoSe_2$	*N_2	-1.596	-1.585	training
MnRu/$MoSe_2$	*NH_2	-2.580	-2.675	training
MnRu/$MoSe_2$	*N_2H	-0.962	-0.980	training
MnRu/$MoSe_2$	*NH_3	-2.353	-2.349	test
MnTa/$MoSe_2$	*NH_3	-2.310	-2.316	training
MnTa/$MoSe_2$	*N_2H	-0.917	-0.960	training
MnTa/$MoSe_2$	*NH_2	-2.614	-2.648	training
MnTa/$MoSe_2$	*N_2	-1.579	-1.564	training
MnTc/$MoSe_2$	*N_2H	-1.034	-0.957	training
MnTc/$MoSe_2$	*N_2	-1.577	-1.561	training
MnTc/$MoSe_2$	*NH_3	-2.345	-2.299	training
MnTc/$MoSe_2$	*NH_2	-2.573	-2.625	training
MnTi/$MoSe_2$	*N_2H	-0.811	-0.854	training
MnTi/$MoSe_2$	*NH_2	-2.455	-2.539	training
MnTi/$MoSe_2$	*N_2	-1.464	-1.458	training
MnV/$MoSe_2$	*NH_2	-2.515	-2.616	training
MnV/$MoSe_2$	*N_2H	-1.031	-0.949	training
MnV/$MoSe_2$	*NH_3	-2.362	-2.266	test
MnV/$MoSe_2$	*N_2	-1.552	-1.553	test
MnW/$MoSe_2$	*N_2	-1.584	-1.558	training
MnW/$MoSe_2$	*NH_2	-2.505	-2.576	training
MnW/$MoSe_2$	*NH_3	-2.210	-2.287	training
MnW/$MoSe_2$	*N_2H	-0.953	-0.954	training
MnY/$MoSe_2$	*NH_2	-2.471	-2.631	training
MnY/$MoSe_2$	*NH_3	-2.285	-2.299	training
MnY/$MoSe_2$	*N_2H	-0.972	-0.986	training
MnY/$MoSe_2$	*N_2	-1.647	-1.588	test
MnZn/$MoSe_2$	*NH_3	-2.392	-2.349	training
MnZn/$MoSe_2$	*N_2	-1.498	-1.523	training
MnZn/$MoSe_2$	*NH_2	-2.601	-2.654	training
MnZr/$MoSe_2$	*NH_2	-2.567	-2.637	training
MnZr/$MoSe_2$	*N_2	-1.640	-1.590	training
MnZr/$MoSe_2$	*NH_3	-2.351	-2.305	training
MnZr/$MoSe_2$	*N_2H	-1.030	-0.986	training
MoFe/$MoSe_2$	*NH_3	-2.466	-2.480	test
MoMn/$MoSe_2$	*N_2	-1.448	-1.600	training
MoMn/$MoSe_2$	*N_2H	-0.965	-1.159	test
MoTi/$MoSe_2$	*NH_3	-1.498	-2.241	test

MoV/$MoSe_2$	*N_2	-1.543	-1.661	test
MoV/$MoSe_2$	*N_2H	-1.074	-1.220	test
NbMn/$MoSe_2$	*NH_3	-2.191	-2.243	training
NbMn/$MoSe_2$	*N_2	-1.096	-1.137	training
NbMn/$MoSe_2$	*N_2H	-0.668	-0.642	training
NbTi/$MoSe_2$	*NH_2	-3.021	-2.836	training
NbTi/$MoSe_2$	*N_2H	-0.565	-0.580	training
NbTi/$MoSe_2$	*N_2	-1.101	-1.076	training
NbTi/$MoSe_2$	*NH_3	-2.264	-2.199	test
NbV/$MoSe_2$	*N_2H	-0.720	-0.653	training
NbV/$MoSe_2$	*N_2	-1.152	-1.148	training
NbV/$MoSe_2$	*NH_3	-2.141	-2.230	training
OsFe/$MoSe_2$	*NH_2	-2.884	-2.821	training
OsFe/$MoSe_2$	*N_2	-2.038	-1.865	training
OsSc/$MoSe_2$	*NH_3	-3.206	-3.245	training
OsSc/$MoSe_2$	*NH_2	-3.602	-3.292	test
OsTi/$MoSe_2$	*N_2	-1.638	-1.639	training
OsV/$MoSe_2$	*N_2	-1.809	-1.735	training
OsV/$MoSe_2$	*NH_3	-2.513	-2.630	training
OsV/$MoSe_2$	*N_2H	-1.225	-1.233	training
ReFe/$MoSe_2$	*N_2H	-1.589	-1.538	training
ReFe/$MoSe_2$	*NH_2	-3.448	-3.052	test
ReFe/$MoSe_2$	*NH_3	-2.750	-2.737	test
ReSc/$MoSe_2$	*NH_3	-3.568	-3.631	training
ReSc/$MoSe_2$	*N_2	-2.711	-2.674	training
ReSc/$MoSe_2$	*NH_2	-4.289	-3.985	training
ReSc/$MoSe_2$	*N_2H	-2.187	-2.254	training
ReTi/$MoSe_2$	*NH_3	-2.112	-2.276	training
ReV/$MoSe_2$	*N_2H	-1.449	-1.451	training
ReV/$MoSe_2$	*NH_3	-2.701	-2.619	training
ReV/$MoSe_2$	*N_2	-1.895	-1.872	training
RhCo/$MoSe_2$	*NH_3	-1.856	-1.832	training
RhCo/$MoSe_2$	*N_2	-0.947	-0.932	training
RhFe/$MoSe_2$	*N_2	-0.966	-0.987	training
RhMn/$MoSe_2$	*NH_3	-1.693	-1.716	training
RhMn/$MoSe_2$	*N_2	-0.722	-0.837	training
RuFe/$MoSe_2$	*N_2H	-0.797	-0.894	training
RuFe/$MoSe_2$	*N_2	-1.535	-1.541	test
RuMn/$MoSe_2$	*NH_3	-2.081	-2.030	training
RuMn/$MoSe_2$	*NH_2	-2.013	-2.031	training
ScAg/$MoSe_2$	*NH_3	-2.549	-2.437	training
ScAg/$MoSe_2$	*N_2	-0.874	-0.772	training
ScAg/$MoSe_2$	*N_2H	-0.314	-0.408	training
ScCd/$MoSe_2$	*NH_2	-2.895	-2.933	training
ScCd/$MoSe_2$	*N_2H	0.156	-0.266	test
ScCu/$MoSe_2$	*N_2	-0.340	-0.509	training

ScCu/$MoSe_2$	*NH_2	-2.877	-2.833	training
ScZn/$MoSe_2$	*NH_2	-2.931	-2.926	training
ScZn/$MoSe_2$	*N_2H	0.250	-0.259	test
TaFe/$MoSe_2$	*N_2H	-1.235	-1.135	training
TaSc/$MoSe_2$	*N_2	-2.199	-2.095	training
TaTi/$MoSe_2$	*N_2H	-0.820	-0.945	training
TaTi/$MoSe_2$	*NH_2	-2.952	-2.766	test
TaV/$MoSe_2$	*N_2H	-1.172	-1.069	training
TaV/$MoSe_2$	*NH_3	-2.458	-2.421	training
TcFe/$MoSe_2$	*NH_2	-2.834	-2.733	training
TcFe/$MoSe_2$	*N_2	-1.648	-1.593	training
TcFe/$MoSe_2$	*NH_3	-2.430	-2.390	training
TcMn/$MoSe_2$	*N_2	-1.492	-1.527	training
TcSc/$MoSe_2$	*NH_2	-2.555	-2.657	training
TiAg/$MoSe_2$	*N_2H	-0.373	-0.448	training
TiAg/$MoSe_2$	*N_2	-1.040	-0.942	training
TiAg/$MoSe_2$	*NH_3	-2.228	-2.297	training
TiAg/$MoSe_2$	*NH_2	-3.040	-2.931	test
TiCr/$MoSe_2$	*NH_2	-2.953	-2.849	training
TiCr/$MoSe_2$	*N_2H	-0.494	-0.405	training
TiCr/$MoSe_2$	*NH_3	-2.122	-2.191	training
TiCr/$MoSe_2$	*N_2	-1.037	-0.898	training
TiCu/$MoSe_2$	*N_2	-0.883	-0.866	training
TiCu/$MoSe_2$	*NH_2	-2.999	-2.847	training
TiCu/$MoSe_2$	*NH_3	-2.191	-2.220	training
TiCu/$MoSe_2$	*N_2H	-0.252	-0.349	training
TiHg/$MoSe_2$	*N_2H	-0.332	-0.437	training
TiHg/$MoSe_2$	*NH_3	-2.292	-2.305	training
TiHg/$MoSe_2$	*NH_2	-3.028	-2.939	training
TiHg/$MoSe_2$	*N_2	-0.988	-0.930	test
TiIr/$MoSe_2$	*N_2H	-0.277	-0.423	training
TiIr/$MoSe_2$	*NH_2	-2.917	-2.917	test
TiMn/$MoSe_2$	*NH_3	-2.190	-2.196	test
TiMo/$MoSe_2$	*N_2	-0.397	-0.648	training
TiMo/$MoSe_2$	*NH_2	-2.376	-2.535	training
TiNi/$MoSe_2$	*NH_3	-2.133	-2.213	training
TiNi/$MoSe_2$	*N_2H	-0.230	-0.349	training
TiNi/$MoSe_2$	*NH_2	-2.973	-2.840	test
TiNi/$MoSe_2$	*N_2	-0.822	-0.843	test
TiOs/$MoSe_2$	*NH_2	-2.901	-2.909	training
TiOs/$MoSe_2$	*N_2	-0.996	-0.924	training
TiOs/$MoSe_2$	*N_2H	-0.483	-0.431	test
TiPt/$MoSe_2$	*NH_2	-2.935	-2.912	training
TiPt/$MoSe_2$	*N_2H	-0.392	-0.418	training
TiPt/$MoSe_2$	*N_2	-0.935	-0.912	training
TiRe/$MoSe_2$	*N_2H	-0.313	-0.332	training

TiRe/$MoSe_2$	*N_2	-0.924	-0.825	training
TiRe/$MoSe_2$	*NH_3	-2.122	-2.121	training
TiRh/$MoSe_2$	*NH_2	-2.991	-2.879	training
TiRh/$MoSe_2$	*NH_3	-2.146	-2.245	training
TiRh/$MoSe_2$	*N_2	-0.740	-0.899	training
TiRh/$MoSe_2$	*N_2H	-0.193	-0.405	test
TiRu/$MoSe_2$	*NH_2	-2.960	-2.895	training
TiRu/$MoSe_2$	*N_2	-0.984	-0.917	training
TiRu/$MoSe_2$	*NH_3	-2.126	-2.261	test
TiTc/$MoSe_2$	*NH_2	-2.994	-2.852	training
TiTc/$MoSe_2$	*N_2H	-0.350	-0.408	training
TiTc/$MoSe_2$	*NH_3	-2.171	-2.218	training
TiV/$MoSe_2$	*NH_2	-2.984	-2.848	training
TiV/$MoSe_2$	*NH_3	-2.054	-2.190	training
TiV/$MoSe_2$	*N_2H	-0.461	-0.404	training
TiZn/$MoSe_2$	*N_2H	-0.446	-0.435	training
TiZn/$MoSe_2$	*NH_3	-2.313	-2.303	training
TiZn/$MoSe_2$	*N_2	-1.112	-0.968	training
TiZr/$MoSe_2$	*N_2	-0.941	-0.918	training
TiZr/$MoSe_2$	*N_2H	-0.409	-0.425	training
TiZr/$MoSe_2$	*NH_3	-2.058	-2.229	test
VAg/$MoSe_2$	*N_2	-1.531	-1.507	training
VAg/$MoSe_2$	*N_2H	-1.035	-0.992	training
VAg/$MoSe_2$	*NH_2	-3.293	-3.141	training
VAg/$MoSe_2$	*NH_3	-2.543	-2.518	training
VCd/$MoSe_2$	*N_2	-1.350	-1.323	training
VCd/$MoSe_2$	*NH_2	-3.185	-2.986	test
VCd/$MoSe_2$	*NH_3	-2.483	-2.399	test
VCo/$MoSe_2$	*NH_3	-2.396	-2.386	training
VCo/$MoSe_2$	*N_2H	-0.816	-0.838	training
VCo/$MoSe_2$	*N_2	-1.330	-1.353	training
VCo/$MoSe_2$	*NH_2	-3.054	-2.995	test
VCu/$MoSe_2$	*N_2	-1.115	-1.231	training
VCu/$MoSe_2$	*N_2H	-0.717	-0.741	training
VCu/$MoSe_2$	*NH_2	-3.022	-2.905	training
VCu/$MoSe_2$	*NH_3	-2.248	-2.325	training
VHf/$MoSe_2$	*N_2H	-0.903	-0.916	training
VHf/$MoSe_2$	*N_2	-1.430	-1.431	test
VHf/$MoSe_2$	*NH_3	-2.381	-2.399	test
VHf/$MoSe_2$	*NH_2	-3.163	-3.026	test
VHg/$MoSe_2$	*NH_3	-2.449	-2.519	training
VHg/$MoSe_2$	*NH_2	-3.198	-3.142	training
VHg/$MoSe_2$	*N_2H	-0.944	-0.973	test
VHg/$MoSe_2$	*N_2	-1.373	-1.488	test
VIr/$MoSe_2$	*NH_3	-2.403	-2.454	training
VIr/$MoSe_2$	*NH_2	-3.074	-3.077	training

VIr/MoSe$_2$	*N_2H	-0.848	-0.917	test
VLa/MoSe$_2$	*NH_3	-2.278	-2.413	training
VLa/MoSe$_2$	*N_2H	-0.915	-0.939	training
VLa/MoSe$_2$	*NH_2	-3.204	-3.041	training
VLa/MoSe$_2$	*N_2	-1.460	-1.454	training
VMn/MoSe$_2$	*N_2	-1.439	-1.396	training
VMn/MoSe$_2$	*NH_3	-2.406	-2.376	training
VMn/MoSe$_2$	*N_2H	-0.935	-0.881	test
VMn/MoSe$_2$	*NH_2	-3.044	-2.991	test
VMo/MoSe$_2$	*NH_3	-2.422	-2.357	training
VMo/MoSe$_2$	*N_2H	-0.916	-0.874	training
VMo/MoSe$_2$	*N_2	-1.424	-1.389	training
VMo/MoSe$_2$	*NH_2	-3.149	-2.937	test
VNi/MoSe$_2$	*N_2	-1.253	-1.342	training
VNi/MoSe$_2$	*N_2H	-0.744	-0.827	training
VNi/MoSe$_2$	*NH_3	-2.372	-2.374	training
VNi/MoSe$_2$	*NH_2	-3.158	-2.983	test
VOs/MoSe$_2$	*NH_2	-2.999	-3.068	training
VOs/MoSe$_2$	*N_2H	-0.881	-0.924	training
VOs/MoSe$_2$	*N_2	-1.356	-1.439	training
VOs/MoSe$_2$	*NH_3	-2.337	-2.457	test
VPd/MoSe$_2$	*N_2H	-1.035	-0.990	training
VPd/MoSe$_2$	*NH_2	-3.255	-3.159	training
VPt/MoSe$_2$	*N_2	-1.347	-1.427	training
VPt/MoSe$_2$	*NH_3	-2.421	-2.449	training
VPt/MoSe$_2$	*NH_2	-3.138	-3.072	training
VPt/MoSe$_2$	*N_2H	-0.980	-0.912	training
VRe/MoSe$_2$	*N_2H	-0.889	-0.868	training
VRe/MoSe$_2$	*N_2	-1.319	-1.383	training
VRe/MoSe$_2$	*NH_3	-2.352	-2.352	training
VRe/MoSe$_2$	*NH_2	-3.037	-2.931	test
VRu/MoSe$_2$	*N_2H	-0.972	-0.917	training
VRu/MoSe$_2$	*NH_3	-2.407	-2.438	training
VRu/MoSe$_2$	*NH_2	-3.073	-3.054	training
VRu/MoSe$_2$	*N_2	-1.360	-1.432	test
VSc/MoSe$_2$	*N_2	-1.418	-1.436	training
VSc/MoSe$_2$	*NH_3	-2.408	-2.393	test
VTa/MoSe$_2$	*NH_3	-2.399	-2.408	training
VTa/MoSe$_2$	*NH_2	-3.149	-3.036	training
VTa/MoSe$_2$	*N_2H	-0.885	-0.906	test
VTa/MoSe$_2$	*N_2	-1.443	-1.421	test
VTc/MoSe$_2$	*N_2H	-0.964	-0.897	training
VTc/MoSe$_2$	*NH_3	-2.389	-2.391	training
VTc/MoSe$_2$	*N_2	-1.462	-1.412	test
VTc/MoSe$_2$	*NH_2	-3.124	-3.007	test
VTi/MoSe$_2$	*N_2H	-0.808	-0.805	training

VTi/MoSe$_2$	*N_2	-1.318	-1.320	training
VTi/MoSe$_2$	*NH_2	-2.982	-2.932	training
VTi/MoSe$_2$	*NH_3	-2.258	-2.316	test
VY/MoSe$_2$	*N_2H	-1.002	-0.948	training
VY/MoSe$_2$	*NH_2	-3.182	-3.041	training
VY/MoSe$_2$	*N_2	-1.495	-1.463	training
VY/MoSe$_2$	*NH_3	-2.364	-2.413	training
VZn/MoSe$_2$	*N_2	-1.245	-1.316	training
VZn/MoSe$_2$	*NH_3	-2.310	-2.391	training
VZn/MoSe$_2$	*NH_2	-2.989	-2.978	training
VZr/MoSe$_2$	*NH_2	-3.179	-3.028	training
VZr/MoSe$_2$	*NH_3	-2.332	-2.400	training
VZr/MoSe$_2$	*N_2H	-0.996	-0.935	training
VZr/MoSe$_2$	*N_2	-1.537	-1.450	test
WFe/MoSe$_2$	*N_2	-1.857	-1.933	training
WFe/MoSe$_2$	*NH_3	-2.690	-2.720	training
WV/MoSe$_2$	*N_2	-1.895	-1.854	training
WV/MoSe$_2$	*NH_3	-2.659	-2.614	training
WV/MoSe$_2$	*N_2H	-1.307	-1.427	training
YTi/MoSe$_2$	*NH_3	-2.526	-2.340	training
YTi/MoSe$_2$	*N_2	-0.519	-0.599	training
ZrMn/MoSe$_2$	*NH_3	-2.185	-2.283	training
ZrMn/MoSe$_2$	*N_2H	-0.532	-0.646	training
ZrMn/MoSe$_2$	*N_2	-1.177	-1.011	training
ZrTi/MoSe$_2$	*N_2	-0.838	-0.935	training
ZrTi/MoSe$_2$	*N_2H	-0.236	-0.569	test
ZrV/MoSe$_2$	*N_2	-1.125	-1.012	training
ZrV/MoSe$_2$	*N_2H	-0.535	-0.646	training
ZrV/MoSe$_2$	*NH_3	-2.204	-2.260	training

Table S2 Catalysts which stand out after two screenings and their adsorption energy of intermediates and free energy of intermediate steps.

Catalyst	$E(N_2)$ /eV	$E(N_2H)$ /eV	$E(NH_2)$ /eV	$E(NH_3)$ /eV	$\Delta G(N_2$-$N_2H)$ /eV	$\Delta G(NH_2$-$NH_3)$ /eV	$\Delta G_{des}(NH_3)$ /eV
CrMn/MoSe$_2$	-1.112	-0.712	-2.899	-2.308	0.401	0.591	1.075
CrZr/MoSe$_2$	-1.122	-0.721	-2.904	-2.313	0.401	0.591	1.080
CrTc/MoSe$_2$	-1.122	-0.721	-2.911	-2.324	0.401	0.587	1.091
CrHf/MoSe$_2$	-1.117	-0.717	-2.904	-2.313	0.401	0.591	1.080
CrTa/MoSe$_2$	-1.124	-0.715	-2.905	-2.323	0.409	0.582	1.090
CrRe/MoSe$_2$	-1.052	-0.645	-2.832	-2.245	0.407	0.587	1.012
CrNi/MoSe$_2$	-1.090	-0.679	-2.904	-2.317	0.411	0.587	1.084
CrFe/MoSe$_2$	-1.715	-1.236	-2.912	-2.446	0.479	0.465	0.508
TcFe/MoSe$_2$	-1.648	-1.284	-2.834	-2.430	0.364	0.404	0.492
OsFe/MoSe$_2$	-2.038	-1.592	-2.884	-2.603	0.445	0.281	0.665
TcMn/MoSe$_2$	-1.492	-1.050	-2.813	-2.356	0.442	0.457	0.418

Table S3 Comparison of the predicted free energy and the calculated free energy of three catalysts verified by DFT.

Catalyst	$E(N_2)$	$E(N_2H)$	$E(NH_2)$	$E(NH_3)$	$\Delta G(N_2\text{-}N_2H)$	$\Delta G(NH_2\text{-}NH_3)$	$\Delta G_{des}(NH_3)$
CrNi/$MoSe_2$	-1.090	-0.679	-2.904	-2.317	0.411	0.587	0.665
DFT	-1.272	-0.855	-2.544	-2.094	0.417	0.450	0.861
OsFe/$MoSe_2$	-2.038	-1.592	-2.884	-2.603	0.445	0.281	1.084
DFT	-1.843	-1.401	-2.788	-2.315	0.442	0.472	1.082
TcMn/$MoSe_2$	-1.492	-1.050	-2.813	-2.356	0.442	0.457	0.418
DFT	-1.520	-1.129	-2.604	-2.102	0.391	0.502	0.869

Supplementary References

1. J. P. Perdew, K. Burke and M. Ernzerhof, *Phys. Rev. Lett.*, 1996, **77**, 3865-3868.
2. G. Kresse and J. Furthmüller, *Physical Review B*, 1996, **54**, 11169-11186.
3. G. Kresse and J. Furthmüller, *Comput. Mater. Sci*, 1996, **6**, 15-50.
4. G. Kresse and D. Joubert, *Physical Review B*, 1999, **59**, 1758-1775.
5. M. Cococcioni and S. de Gironcoli, *Physical Review B*, 2005, **71**, 035105.
6. M. Khan, M. N. Tripathi and A. Tripathi, *Mater. Sci. Semicond. Process.*, 2024, **177**, 108339.
7. M. Khan, M. N. Tripathi and A. Tripathi, *J. Mater. Res.*, 2022, **37**, 3340-3351.
8. E. Skulason, T. Bligaard, S. Gudmundsdottir, F. Studt, J. Rossmeisl, F. Abild-Pedersen, T. Vegge, H. Jonsson and J. K. Norskov, *Phys. Chem. Chem. Phys.*, 2012, **14**, 1235-1245.
9. J. G. Howalt, T. Bligaard, J. Rossmeisl and T. Vegge, *Phys. Chem. Chem. Phys.*, 2013, **15**, 7785-7795.
10. L. Breiman, *Mach. Learn.*, 1996, **24**, 123-140.
11. F. Pedregosa, G. Varoquaux, A. Gramfort, V. Michel, B. Thirion, O. Grisel, M. Blondel, P. Prettenhofer, R. Weiss, V. Dubourg, J. Vanderplas, A. Passos, D. Cournapeau, M. Brucher, M. Perrot and E. Duchesnay, *J. Mach. Learn. Res.*, 2011, **12**, 2825-2830.
12. A. C. Lorena, L. F. O. Jacintho, M. F. Siqueira, R. D. Giovanni, L. G. Lohmann, A. C. P. L. F. de Carvalho and M. Yamamoto, *Expert Syst. Appl.*, 2011, **38**, 5268-5275.
13. J. H. Friedman, *The Annals of Statistics*, 2001, **29**, 1189-1232.